Can *GW* handle multireference systems?

Abdallah Ammar ; Antoine Marie ; Mauricio Rodríguez-Mayorga ; Hugh G. A. Burton ;
Pierre-François Loos

Check for updates

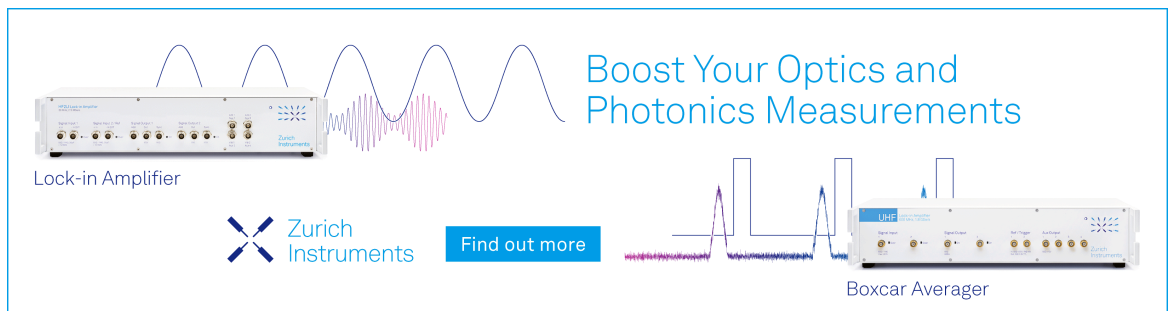View Online

Export Citation

CrossMark

AIP
Publishing

Can *GW* handle multireference systems?

View Online   Export Citation   CrossMark

Abdallah Ammar,[1,a] (ID) Antoine Marie,[1,b] (ID) Mauricio Rodríguez-Mayorga,[2,c] (ID) Hugh G. A. Burton,[3,d] (ID) and Pierre-François Loos[1,e] (ID)

AFFILIATIONS

[1] Laboratoire de Chimie et Physique Quantiques (UMR 5626), Université de Toulouse, CNRS, UPS, Toulouse, France
[2] Université Grenoble Alpes, CNRS, Institut NEEL, F-38042 Grenoble, France
[3] Yusuf Hamied Department of Chemistry, University of Cambridge, Lensfield Road, Cambridge CB2 1EW, United Kingdom

[a] Electronic mail: aammar@irsamc.ups-tlse.fr
[b] Electronic mail: amarie@irsamc.ups-tlse.fr
[c] Electronic mail: marm3.14@gmail.com
[d] Electronic mail: hgaburton@gmail.com
[e] Author to whom correspondence should be addressed: loos@irsamc.ups-tlse.fr

ABSTRACT

Due to the infinite summation of bubble diagrams, the *GW* approximation of Green's function perturbation theory has proven particularly effective in the weak correlation regime, where this family of Feynman diagrams is important. However, the performance of *GW* in multireference molecular systems, characterized by strong electron correlation, remains relatively unexplored. In the present study, we investigate the ability of *GW* to handle closed-shell multireference systems in their singlet ground state by examining four paradigmatic scenarios. First, we analyze a prototypical example of a chemical reaction involving strong correlation: the potential energy curve of BeH_2 during the insertion of a beryllium atom into a hydrogen molecule. Second, we compute the electron detachment and attachment energies of a set of molecules that exhibit a variable degree of multireference character at their respective equilibrium geometries: LiF, BeO, BN, C_2, B_2, and O_3. Third, we consider a H_6 cluster with a triangular arrangement, which features a notable degree of spin frustration. Finally, the dissociation curve of the HF molecule is studied as an example of single bond breaking. These investigations highlight a nuanced perspective on the performance of *GW* for strong correlation depending on the level of self-consistency, the choice of initial guess, and the presence of spin-symmetry breaking at the Hartree–Fock level.

Published under an exclusive license by AIP Publishing. https://doi.org/10.1063/5.0196561

I. INTRODUCTION

The *GW* approximation of many-body perturbation theory, as proposed by Hedin,[1] can be regarded as the workhorse of Green's function methods,[2] as the vast majority of contemporary calculations performed within this theoretical framework are conducted using the *GW* approximation. The importance of *GW* is evident in the solid-state community[3–5] and its influence is now extending to quantum chemistry, where *GW* has experienced a substantial surge in popularity over the past decade.[6,7]

This widespread adoption can, in part, be ascribed to the emergence of electronic structure packages that provide efficient implementations of the *GW* equations,[8–29] enabling calculations on large-scale molecular systems.[12,13,15,21,22,30–37] These software packages have been bolstered by the creation of well-curated and accurate reference values, such as the *GW*100 dataset of van Setten and

collaborators,[38] which reports ionization potentials (IPs) and electron affinities (EAs) for 100 small- and medium-sized closed-shell molecules containing a variety of elements and chemical bonds (see also Refs. 39–46). Similar arguments[11,18,47–69] can be put forward for formalisms based on the Bethe–Salpeter equations.[11,62,70,71]

GW is often hailed as "miraculously" accurate for weakly correlated systems, given its quite reasonable computation cost.[72] However, it is usually considered inadequate for strongly correlated materials.[73–80] This perception arises because the *GW* self-energy is constructed based on a polarizability computed as an infinite summation of a specific class of diagrams, known as bubble diagrams,[81,82] which are recognized to be relevant primarily in the weakly correlated regime.[83–89] In this context, the term "strong correlation" denotes a specific form of electron correlation observed, for example, in transition metal oxides (such as Mott insulators[90,91]), the large-U limit of the Hubbard model,[92–94] or the

low-density regime of the uniform electron gas[95,96] (where Wigner crystals are formed[97]). Therefore, the assessment of *GW* and the definition of strong correlation are specifically rooted in strongly correlated systems pertinent to the condensed matter community. The objective of this work is to evaluate whether this assessment stands for strongly correlated systems encountered in quantum chemistry.

Before introducing the systems that we studied to address this question, let us mention that alternative approximations based on Green's functions do exist and have been studied in the strong correlation regime. The *T*-matrix[80,98–109] approximation is based on an alternative infinite summation to the one used to build the *GW* polarizability, namely, a summation of ladder diagrams.[80,110–112] This resummation is justified in the low-density limit of the uniform electron gas with short-range interactions.[82] It is not clear whether this resummation is adapted to single- or multi-reference molecular systems, where the long-range Coulomb interaction is ubiquitous. Numerous groups have proposed strategies to go beyond the *GW* approximation, but these have their own theoretical and practical challenges.[19,72,104,113–130]

In the present context, strong correlation specifically refers to molecular systems where multiple electronic configurations are nearly degenerate; thus, strong correlation is synonymous with static correlation. A system is considered strongly correlated if there is more than one electronic configuration with a significant weight in the configuration interaction (CI) expansion. Crucially, this definition is contingent on the choice of the underlying orbitals used to construct these electronic configurations, which further blurs the demarcation between weak and strong correlation. Hence, it is not surprising that several diagnostics have been developed to measure multireference character in different contexts.[131–137] Furthermore, we differentiate between two types of systems: the first exhibits multireference character exclusively in excited states, while the second involves multireference character in the reference wave function, possibly extending to excited states. This study primarily addresses the more challenging second case.

We explore the capability of the *GW* approximation to handle such closed-shell multireference systems in their singlet ground state. To assess this, we examine four distinct quantum chemistry scenarios involving such systems. First, we analyze the potential energy curve of BeH_2 during the insertion of a beryllium atom into a hydrogen molecule, resulting in the linear BeH_2 molecule.[138] This system serves as a prototypical example of strong correlation and has been extensively studied by various authors in different contexts.[139–150] Second, we compute the properties of a set of molecules exhibiting, at their respective equilibrium geometries, a variable degree of multireference character. Third, we investigate the H_6 system arranged in a triangular configuration, a system showing a significant amount of spin frustration. Finally, the evolution of the principal IP of the HF molecule is studied during its dissociation, which is a stringent test due to the varying amount of dynamical and static correlations as a function of the bond length.[149,151–158] Our key findings reveal a nuanced perspective on the capabilities of *GW* in describing multireference systems, indicating that it does possess a certain ability to capture their complex electronic structure. Unless otherwise stated, atomic units are used.

II. A PRIMER ON *GW*

Here, we report the set of equations required to understand and apply the *GW* formalism and refer the interested reader to dedicated reviews[3–7] and books[2,103,159,160] for additional information.

In the four-point formalism,[80,121,161] the instantaneous Coulomb potential is defined as

$$v(12;1'2') = \delta(11')\frac{\delta(t_1 - t_2)}{|\mathbf{r}_1 - \mathbf{r}_2|}\delta(22'). \tag{1}$$

Here, $\delta(11')$ is the Dirac function, and the integers, e.g., 1, serve as shorthand notations for time (t_1) and spin-space $\mathbf{x}_1 = (\sigma_1, \mathbf{r}_1)$ variables for each particle.

In practice, within the *GW* approximation, we initiate the process by considering a reference propagator G_0, typically derived from a mean-field model. Therefore, we directly present the coupled integro-differential equations governing the *GW* formalism for $G_0 = G_{HF}$. The total self-energy is represented as a sum of the Hartree (H), exchange (x), and correlation (c) self-energies such that

$$\Sigma(11') = \Sigma_H(11') + \Sigma_x(11') + \Sigma_c(11'). \tag{2}$$

The exchange–correlation part, $\Sigma_{xc} = \Sigma_x + \Sigma_c$, is expressed as a convolution of the interacting Green's function G and the dynamically screened Coulomb interaction W,

$$\Sigma_{xc}(11') = i \int d(22')G(22')W(12';21'), \tag{3}$$

where W is determined by the irreducible polarizability $\tilde{L}$, as follows:

$$W(12;1'2') = v(12^-;1'2') - i \int d(343'4')W(14;1'4') \\ \times \tilde{L}(3'4';3^+4)v(23;2'3'). \tag{4}$$

A sign over an integer, denoted as, for example, $1^\pm$, indicates an infinitesimal time shift $t_{1^\pm} = t_1 \pm \eta$. In the *GW* framework, the irreducible polarizability is approximated by the product of two Green's functions,

$$\tilde{L}(12;1'2') = G(12')G(21'), \tag{5}$$

while the one-body Green's function G is obtained through a Dyson equation,

$$G(11') = G_{HF}(11') + \int d(22')G_{HF}(12)\Sigma_c(22')G(2'1'). \tag{6}$$

In practical applications, it is advantageous to introduce a set of real-valued spin-orbital basis functions, denoted as $\{\varphi_p\}$, with corresponding energies $\{\epsilon_p\}$ for describing quasiparticles. This approach enables us to write down the Lehmann representation of G in the following manner:

$$G(\mathbf{x}_1\mathbf{x}_{1'};\omega) = \sum_i \frac{\varphi_i(\mathbf{x}_1)\varphi_i(\mathbf{x}_{1'})}{\omega - \epsilon_i - i\eta} + \sum_a \frac{\varphi_a(\mathbf{x}_1)\varphi_a(\mathbf{x}_{1'})}{\omega - \epsilon_a + i\eta}. \tag{7}$$

Here, we follow the common practice of using $a, b, \ldots$ to represent states above the Fermi level (virtual orbitals) and $i, j, \ldots$ for states below (occupied orbitals). The indices $p, q, \ldots$ denote arbitrary (i.e.,

occupied or virtual) orbitals. The calculation of quasiparticle energies and their corresponding Dyson orbitals will be the focus of the upcoming discussion.

Performing various Fourier transforms and projecting onto the spin orbital basis enable us to derive the analytical expression of the matrix elements associated with the correlation part of the self-energy,

$$[\Sigma_c(\omega)]_{pq} = \sum_{mi} \frac{M_{pi}^m M_{qi}^m}{\omega + \Omega_m - \epsilon_i - \imath\eta} + \sum_{ma} \frac{M_{pa}^m M_{qa}^m}{\omega - \Omega_m - \epsilon_a + \imath\eta}, \quad (8)$$

where we have introduced the elements of the transition densities,

$$M_{pq}^m = \sum_{ia} \langle pi|qa\rangle \left(X_{ia}^m + Y_{ia}^m\right). \quad (9)$$

The braket notation is employed to represent the bare two-electron Coulomb integrals,

$$\langle pq|rs\rangle = \iint \frac{\varphi_p(\mathbf{x}_1)\varphi_q(\mathbf{x}_2)\varphi_r(\mathbf{x}_1)\varphi_s(\mathbf{x}_2)}{|\mathbf{r}_1 - \mathbf{r}_2|} d\mathbf{x}_1 d\mathbf{x}_2. \quad (10)$$

The excitation energies Ω_m and amplitudes X_{ia}^m, Y_{ia}^m are obtained as eigenvalues and eigenvectors of a Casida-like eigenproblem,

$$\begin{pmatrix} A & B \\ -B & -A \end{pmatrix} \begin{pmatrix} X_m \\ Y_m \end{pmatrix} = \Omega_m \begin{pmatrix} X_m \\ Y_m \end{pmatrix}, \quad (11)$$

where

$$A_{ia,jb} = (\epsilon_a - \epsilon_i)\delta_{ij}\delta_{ab} + \langle ib|aj\rangle,$$
$$B_{ia,jb} = \langle ij|ab\rangle. \quad (12)$$

We now shift our focus to the computation of the Dyson orbitals $\{\varphi_p\}$ and quasiparticle energies $\{\epsilon_p\}$. The Dyson equation [Eq. (6)] implies that these quantities should satisfy the following dynamical non-Hermitian equation:

$$[F + \Sigma_c(\omega = \epsilon_p)]\varphi_p = \epsilon_p \varphi_p, \quad (13)$$

where F is the Fock operator. However, the frequency dependence of the correlation self-energy Σ_c introduces complexity and non-linearity to this quasiparticle equation. As a result, various common approximations are employed. The widely used G_0W_0 scheme involves a single iteration of Eq. (13), considering only the diagonal part of the self-energy.[162–168] For instance, starting with a set of one-electron HF orbitals $\{\varphi_p^{HF}\}$, where $F\varphi_p^{HF} = \epsilon_p^{HF}\varphi_p^{HF}$, the following equations are obtained and solved:

$$\epsilon_p^{HF} + [\Sigma_c(\omega)]_{pp} = \omega. \quad (14)$$

Linearizing this equation is a common practice, achieved by performing a first-order Taylor expansion of the self-energy around $\omega = \epsilon_p^{HF}$. An iterative approach, known as evGW, goes a step further by updating the eigenvectors X_m, Y_m, and eigenvalues Ω_m, and consequently updating the self-energy, until convergence over the quasiparticle energies $\{\epsilon_p\}$ is achieved.[8,169–172] The qsGW method introduces another level of self-consistency, where both orbitals and energies are iteratively updated until convergence.[17,21,60,173–177] However, to avoid dealing with the non-Hermitian and dynamical

nature of the correlation self-energy, a static symmetric approximation is considered instead, which reads

$$\langle\varphi_p|F|\varphi_q\rangle + \frac{[\Sigma_c(\epsilon_p)]_{pq} + [\Sigma_c(\epsilon_q)]_{qp}}{2} = \epsilon_p \delta_{pq}. \quad (15)$$

Recently, a qsGW scheme based on a static Hermitian self-energy obtained from a similarity renormalization group approach has been proposed as an alternative to Eq. (15).[177]

Based on these calculations, the principal IP and EA of a given system are obtained as

$$IP = -\epsilon_{HOMO}, \qquad EA = -\epsilon_{LUMO}, \quad (16)$$

where HOMO and LUMO are the highest-occupied and lowest-unoccupied molecular orbitals, respectively. These identities are valid at the HF and GW levels.

III. COMPUTATIONAL DETAILS

The reference data specifically produced for the present study have been obtained at the full CI (FCI) level. All these calculations have been performed with QUANTUM PACKAGE[178] using the *"Configuration Interaction using a Perturbative Selection made Iteratively"* (CIPSI) algorithm[179–183] and within the frozen-core approximation.

The GW calculations have been carried out with QUACK, an open-source software for emerging quantum electronic structure methods, for which the source code is available at https://github.com/pfloos/QuAcK. Their algorithm and implementation are described in Ref. 7. In the G_0W_0 and evGW calculations, we set $\eta = 0$ and we solve the frequency-dependent quasiparticle equation without relying on its linearization to get the quasiparticle energies. The qsGW calculations are performed with the regularized scheme based on the similarity renormalization group approach, as mentioned above and described in Ref. 177. A flow parameter of $s = 1000$ is employed. All (occupied and virtual) orbitals are corrected.

The systems considered here have a closed-shell electronic structure, and, unless otherwise stated, we have opted to maintain spatial and spin symmetry. Therefore, we rely on the restricted formalism for the HF and GW calculations. The restricted HF (RHF) calculations are systemically initiated with a core Hamiltonian guess, and an internal stability analysis of the RHF solution toward other RHF solutions is systematically performed.[184–186] All GW calculations employed these RHF quantities as a starting point. A systematic treatment of these systems with more exotic HF formalisms, including the unrestricted and/or generalized approaches, is deferred to future work.[187–191] For each system and method, the raw data are collected in the supplementary material.

IV. RESULTS

A. Be + H₂ reaction

Using a simple Be(3s2p)/H(2s) basis set (see the supplementary material) and correlating all electrons, we initially examine the insertion of a beryllium atom into H_2 to form BeH_2 following a C_{2v} pathway[138] or at least the variant proposed by Evangelista and co-workers.[148–150] As depicted in the left panel of Fig. 1, the Be atom
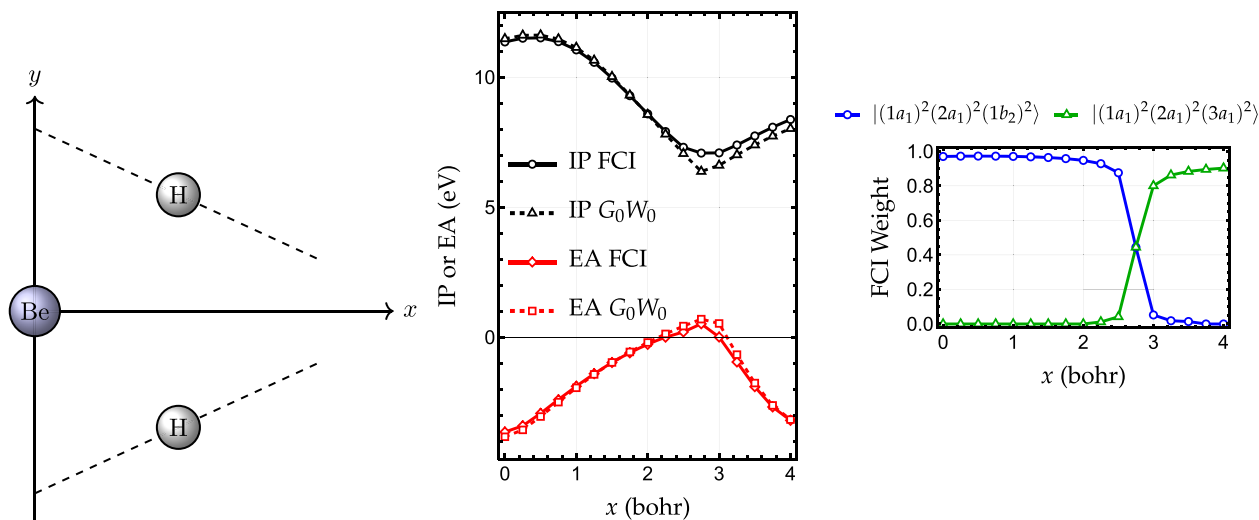
FIG. 1. Left: Sketch of the insertion reaction of Be into H_2. The x coordinate varies from 0 to 4 bohrs, and $y = 2.54-0.46x$. Center: Variations of the principal IP and EA (in eV) during the reaction as functions of x. Right: Evolution of the FCI weights associated with the two dominant electronic configurations, $|(1a_1)^2(2a_1)^2(1b_2)^2\rangle$ and $|(1a_1)^2(2a_1)^2(3a_1)^2\rangle$, as functions of x.

is placed at the center of the coordinate system, and two hydrogen atoms are located at $(x, \pm y, 0)$ with $y = 2.54-0.46x$ and x ranging from 0 to 4 bohrs. At small $x > 0$, the FCI wave function of BeH_2 is dominated by the electronic configuration $|(1a_1)^2(2a_1)^2(1b_2)^2\rangle$, while for larger x, the configuration $|(1a_1)^2(2a_1)^2(3a_1)^2\rangle$ prevails. In the region $2.5 < x < 3$, the wave function switches rapidly from $|(1a_1)^2(2a_1)^2(1b_2)^2\rangle$ to $|(1a_1)^2(2a_1)^2(3a_1)^2\rangle$, as illustrated in the right panel of Fig. 1. Particularly, at $x = 2.75$, the wave function contains an equal amount of the two configurations. This region of strong multireference effects is anticipated to produce the largest deviations between the reference FCI values and the GW-based methods.

To determine the exact IP and EA of this system, we performed FCI calculations on the cation, neutral, and anionic species at each geometry from $x = 0$ to $x = 4$ (central panel of Fig. 1). Starting from $x = 0$, the IP decreases, reaching a minimum at $x = 2.75$, while the EA increases to its maximum at the same point. Additionally, we computed the errors in IP and EA (with respect to FCI) across the entire range of x values using HF, G_0W_0, evGW, and qsGW (see Fig. 2).

At each level of theory, the behavior of the charged excitation energies closely mirrors the FCI results, except around $x = 2.75$, where a significant deviation occurs. At the FCI level, the transition between the two regions is smooth, while at the HF level and hence at the GW level as well, the transition is better described by two solutions crossing abruptly. This behavior is ubiquitous in excited-state HF calculations.[192–194] Overall, Fig. 2 illustrates that GW notably improves upon HF, with G_0W_0 and evGW exhibiting close agreement. In addition, qsGW only improves in the small-x region and does not provide more accurate properties in the problematic region around $x = 2.75$, where all GW methods yield essentially the same values. In the worst-case scenario, GW deviates by 0.7 eV for the IP and 0.5 eV for the EA. Furthermore, the

isolated Be also features a strong competition between the $|(1s)^2(2s)^2\rangle$ and $|(1s)^2(2p)^2\rangle$ configurations.[195] Therefore, the large-x limit of Be + H_2 will also have multireference characteristics, which are evident in the larger errors in the predicted IP for $x > 2.75$. These results highlight that the quality of the HF reference wave function is crucial and that self-consistency does not lead to any significant improvement. Nonetheless, we can conclude that the GW approximation provides a quantitative description of the Be + H_2 reaction, except in the strongly multireference region where the agreement is only qualitative.

Except for $2.75 \leq x \leq 2.9$, the RHF solution remains internally stable (i.e., there is no RHF-to-RHF instability). From $x = 2.75-2.9$, one can find a spatially symmetry-broken RHF solution with energy lower than the symmetry-pure RHF solution. The numerical results
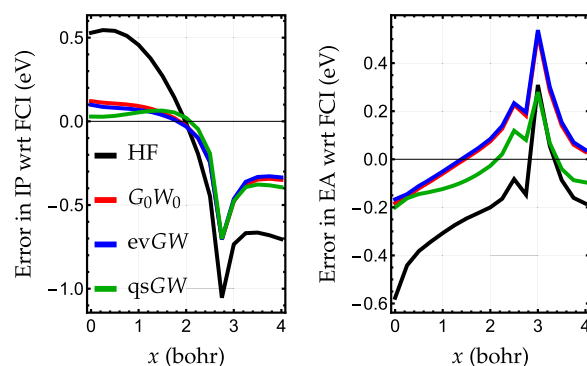

FIG. 2. Error in IP and EA with respect to FCI (in eV) during the insertion reaction of Be into H_2 as a function of x computed at the HF, G_0W_0, evGW, and qsGW levels.
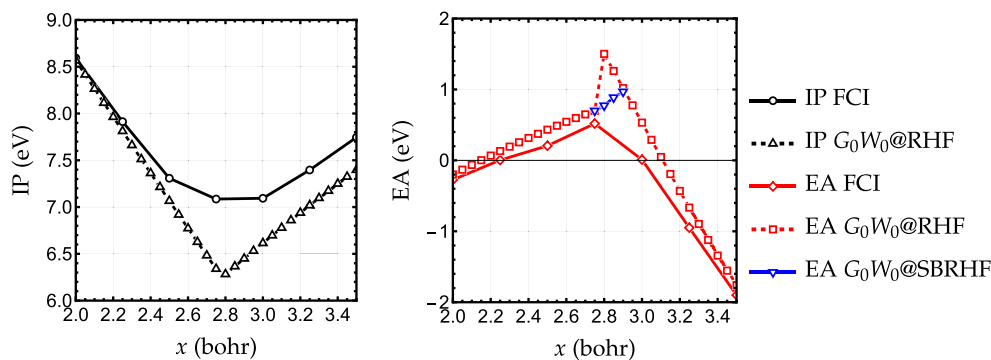
FIG. 3. Variations of the principal IP and EA (in eV) during the reaction in the range $2 \leq x \leq 3.5$ obtained at the FCI (solid curves) and G_0W_0 (dashed lines) levels. The symmetry-pure RHF and spatially symmetry-broken RHF (SBRHF) solutions are considered as starting points for the G_0W_0 calculations. For the IP, the two solutions yield nearly identical results (not shown), while the EA values differ significantly for $2.75 \leq x \leq 2.9$.

obtained with these two solutions are extremely close in the case of the IP (results not shown), while they differ quite significantly for the EA. In Fig. 3, we represent the variation of the IP and EA in the range $2 \leq x \leq 3.5$. The IP and EA values computed with G_0W_0 feature a cusp or discontinuity when the reference RHF state switches abruptly. Furthermore, relying on the broken-symmetry solution has the effect of removing the discontinuity in the EA computed at the G_0W_0 level (blue markers) and provides a better match with the FCI values overall.

B. Multireference systems

In the second stage of this study, we explore a set of molecules exhibiting varying degrees of multireference character, spanning from weakly to strongly multireference systems, each analyzed at its experimentally determined equilibrium geometry.[196] The geometric parameters for these molecules are compiled in Table I. The respective weights of the RHF reference determinant in the cationic, neutral, and anionic singlet ground-state wave functions are reported in Table I. Here, we employ the more realistic triple-ζ basis set, def2-TZVPP.[197]

The boron dimer displays a pronounced multireference character in its lowest singlet state (HF determinant weight of only 0.36) although the true ground state possesses triplet spin

TABLE I. Ground-state geometries (in Å and degrees) of the considered molecular systems, spanning a spectrum from weakly to strongly multireference character, as well as the corresponding weights of the reference configuration in the FCI wave function for the cationic, neutral, and anionic singlet ground states.

System	Geometry	Reference weight		
		Cation	Neutral	Anion
B_2	$R_{BB} = 1.59$	0.73	0.36	0.71
LiF	$R_{LiF} = 1.5639$	0.96	0.93	0.94
BeO	$R_{BeO} = 1.3308$	0.93	0.90	0.94
BN	$R_{BN} = 1.281$	0.69	0.69	0.80
C_2	$R_{CC} = 1.2425$	0.69	0.69	0.82
O_3	$R_{OO} = 1.278$	0.74	0.76	0.76
	$\angle_{OOO} = 116.8$			

symmetry ($^3\Sigma_g^-$), and the corresponding HF wave function has the configuration $|\cdots\sigma_u^2\sigma_g^2\sigma_u^2\pi_u^2\rangle$.[198–201] The carbon dimer serves as a prototypical multireference system (weight of 0.69 on the reference determinant) extensively studied in the literature using state-of-the-art electronic structure methods.[202–206] We also consider other members of the 12-electron series (LiF, BeO, BN, and ozone), which are all part of the GW100 dataset.[38] (Although we consider the lowest-energy singlet state, it is worth noting that BN has a triplet ground state.[207]) Moving from LiF to C_2, the multireference character magnifies. Notably, all these systems exhibit a positive electron affinity, implying the stability of their corresponding anion.

Our results, summarized in Table II, include the IP, EA, and fundamental gap computed at the G_0W_0, evGW, qsGW, and FCI levels of theory. Errors with respect to the reference FCI values are indicated in parentheses. Starting with a core guess, for the more pronounced multireference systems (B_2, BN, and C_2), an internally unstable RHF solution (labeled as No. 1) is obtained. By following the eigenvector associated with the negative eigenvalue, a lower-lying RHF solution labeled as No. 2 is reached (see Table III). For B_2, both RHF solutions have broken spatial symmetry. In C_2, No. 1 has a configuration $|\cdots\sigma_g^2\sigma_u^2\pi_u^2\pi_u^2\rangle$ and is of $^1\Sigma_g^+$ symmetry, while No. 2 has broken spatial symmetry. A similar situation arises in BN, where No. 1 has $^1\Sigma^+$ symmetry and a configuration $|\cdots\sigma^2\sigma^2\pi^2\pi^2\rangle$, while the wave function of No. 2 is spatially broken. For LiF, BeO, and O_3, No. 1 is found to be internally stable. The IP and EA obtained with GW based on No. 1 are very acceptable, but in some cases, improvement can be obtained by considering the lower-energy RHF solution No. 2, as explained further below.

For the IP of B_2, transitioning from No. 1 to No. 2 results in a negative shift of ~0.2 eV. At the G_0W_0 and evGW levels, the exact result falls almost exactly between the quasiparticle energies obtained with the two reference RHF solutions. Consequently, we observe a very small improvement with errors around 0.1 eV, unexpectedly well below the mean absolute error of GW calculated on the GW100 benchmark test set (0.31 eV at the G_0W_0@HF level). Due to self-consistency overcorrecting the IPs, the error in qsGW reaches 0.26 eV when considering No. 2 as the starting point. The errors on the EAs are larger, as expected. Nonetheless, the overall trend is very similar.

TABLE II. Principal IP, principal EA, and fundamental gap (in eV) for a selection of multireference systems computed at the G_0W_0, evGW, qsGW, and FCI levels of theory with the def2-TZVPP basis. No. 1 and No. 2 correspond to distinct RHF solutions whose properties are collected in Table III. The error with respect to the reference FCI value is reported in parentheses.

| Mol. | | G_0W_0 | | evGW | | qsGW | | FCI |
		No. 1	No. 2	No. 1	No. 2	No. 1	No. 2	
B$_2$	IP	9.06 (+0.09)	8.87 (−0.10)	9.10 (+0.13)	8.87 (−0.10)	8.84 (−0.13)	8.71 (−0.26)	8.97
	EA	2.05 (+0.19)	2.13 (+0.27)	2.12 (+0.26)	2.20 (+0.34)	1.90 (+0.04)	2.15 (+0.29)	1.86
	Gap	7.01 (−0.11)	6.74 (−0.37)	6.98 (−0.14)	6.69 (−0.42)	6.94 (−0.18)	6.56 (−0.55)	7.11
LiF	IP	11.31 (−0.01)		11.09 (−0.23)		11.38 (+0.06)		11.32
	EA	0.01 (−0.01)		0.02 (+0.00)		0.00 (−0.02)		0.02
	Gap	11.29 (−0.01)		11.07 (−0.23)		11.38 (+0.08)		11.30
BeO	IP	9.76 (−0.21)		9.63 (−0.34)		10.10 (+0.13)		9.97
	EA	2.09 (+0.12)		2.12 (+0.15)		1.94 (−0.03)		1.97
	Gap	7.67 (−0.32)		7.51 (−0.48)		8.17 (+0.17)		8.00
BN	IP	11.69 (−0.24)	11.90 (−0.03)	11.68 (−0.24)	11.93 (−0.03)	11.83 (−0.10)	11.83 (−0.10)	11.93
	EA	3.83 (+0.84)	3.70 (+0.71)	3.89 (+0.90)	3.76 (+0.77)	3.34 (+0.35)	3.34 (+0.35)	2.99
	Gap	7.86 (−1.08)	8.20 (−0.73)	7.79 (−1.15)	8.17 (−0.79)	8.49 (−0.45)	8.49 (−0.45)	8.94
C$_2$	IP	12.92 (+0.48)	12.42 (−0.03)	12.95 (+0.50)	12.42 (−0.03)	12.54 (+0.09)	12.16 (−0.29)	12.45
	EA	4.08 (+1.08)	4.40 (+1.40)	4.16 (+1.16)	4.48 (+1.48)	3.73 (+0.73)	4.40 (+1.40)	3.00
	Gap	8.85 (−0.60)	8.02 (−1.43)	8.79 (−0.66)	7.93 (−1.52)	8.81 (−0.64)	7.76 (−1.69)	9.45
O$_3$	IP	13.50 (+0.92)		13.40 (+0.82)		13.12 (+0.54)		12.58
	EA	1.96 (+0.68)		2.01 (+0.73)		1.85 (+0.57)		1.28
	Gap	11.54 (+0.25)		11.39 (+0.10)		11.28 (−0.01)		11.29

TABLE III. Properties of the two RHF solutions of B$_2$, BN, and C$_2$ computed with the def2-TZVPP basis. The negative eigenvalues (in E_h) of the internal stability analysis are reported alongside the RHF energy (in E_h), E_{HF}, and the HOMO and LUMO orbital energies (in eV), ϵ_{HOMO}^{HF} and ϵ_{LUMO}^{HF}.

Mol.	Sol.	E_{HF}	Int. Stab.	ϵ_{HOMO}^{HF}	ϵ_{LUMO}^{HF}
B$_2$	No. 1	−49.042 173	−0.043	−8.54	−1.18
	No. 2	−49.059 358		−8.71	−1.05
BN	No. 1	−78.908 465	−0.019	−11.53	−2.93
	No. 2	−78.911 128		−11.16	−2.69
C$_2$	No. 1	−75.403 580	−0.067	−12.46	−3.12
	No. 2	−75.439 770		−12.79	−2.78

It is noteworthy that although qsGW is generally considered independent of the starting point due to self-consistency on quasiparticle energies and corresponding orbitals, initiating the qsGW self-consistent process with No. 1 or No. 2 may lead to different sets of results. As qsGW considers a Fock-like operator, including Hartree, exchange, and correlation (similar to Kohn–Sham calculations), it is not surprising to locate different solutions at the qsGW level. In the case of the carbon dimer, using No. 2 as a starting point significantly improves the IPs for G_0W_0 and evGW, while it deteriorates the qsGW results. Similar observations apply to BN. In particular, considering the lowest-energy RHF solution significantly improves both the IP and EA computed at the G_0W_0 and evGW levels. It is interesting to note that, in the case of BN, starting the qsGW

calculations with No. 1 or No. 2 leads to the same quasiparticle energies, and again, the accuracy reached is quite reasonable.

For the more weakly correlated systems, LiF and BeO, the IPs and EAs are well reproduced by GW, especially at the G_0W_0 and qsGW levels (evGW errors are slightly larger). For O$_3$, which exhibits a more significant multireference character than the two previous systems, errors are larger (up to almost 1 eV for G_0W_0). Nonetheless, the qsGW formalism can significantly reduce these errors. In conclusion, the best compromise appears to be qsGW@RHF using the symmetry-pure solution (No. 1), providing accurate IPs and EAs for the weakly and more strongly correlated systems that are considered here.

For the sake of completeness, we report, in the supplementary material, G_0W_0 results computed with Kohn–Sham starting points (BLYP,[208,209] B3LYP,[208–210] and CAM-B3LYP[211]) for the same set of molecules. The stability analysis reveals that all the considered density-functional approximations lead to a unique stable restricted solution and that only G_0W_0@CAM-B3LYP produces competitive results when compared to G_0W_0@HF.

C. Triangular-shaped H$_6$ cluster

The geometry of the H$_6$ cluster, with a 2 Å separation between each hydrogen atom, is reported in the supplementary material. To simplify the present analysis, we employ the minimal STO-6G basis set. At the FCI/STO-6G level, the ground-state energies for the cation, neutral, and anionic species are −2.516 380E_h, −2.857 023E_h, and −2.664 959E_h, respectively, resulting in an IP and EA of 9.27 eV

TABLE IV. Nature and properties of the different HF solutions located for the triangular-shaped H_6 cluster using the STO-6G basis. The HF energy (in E_h), E_{HF}, and the expectation value of $\hat{S}^2$ are indicated for each solution. The IP and EA (in eV) computed at the HF, G_0W_0, qsGW, and FCI levels are also reported, and the error with respect to the reference FCI value is indicated in parentheses.

				HF		G_0W_0		qsGW		FCI	
Nat.	Sol.	E_{HF}	$\langle \hat{S}^2 \rangle$	IP	EA	IP	EA	IP	EA	IP	EA
RHF		−2.449 047	0.000	6.36 (−2.91)	−3.22 (+2.01)	6.55 (−2.72)	−2.94 (+2.29)	6.48 (−2.79)	−2.86 (+2.37)	9.27	−5.23
UHF	No. 1	−2.798 321	2.821	10.38 (+1.11)	−5.51 (−0.28)	10.09 (+0.82)	−5.28 (−0.05)	10.01 (+0.74)	−5.20 (+0.03)	9.27	−5.23
UHF	No. 2	−2.819 463	2.742	10.42 (+1.15)	−6.92 (−1.69)	10.06 (+0.79)	−6.56 (−1.33)	9.95 (+0.68)	−6.43 (−1.20)	9.27	−5.23
UHF	No. 3	−2.824 460	2.712	11.16 (+1.89)	−6.26 (−1.03)	10.75 (+1.48)	−5.94 (−0.71)	10.61 (+1.34)	−5.84 (−0.61)	9.27	−5.23

and −5.23 eV, respectively. The RHF estimates of the IP and EA deviate significantly from these FCI values, with an offset of ~3 eV for the IP and 2 eV for the EA. Moreover, performing a GW calculation on top of the RHF results does not yield any improvement, and self-consistency has minimal impact, slightly worsening the results.

While the RHF solution is internally stable, it is unstable toward UHF (RHF-to-UHF instabilities). The stability analysis reveals five negative eigenvalues: one non-degenerate at $-0.647E_h$ and two sets of doubly degenerate eigenvalues at $-0.362E_h$ and $-0.079E_h$. Following the lowest eigenvalues leads to the lowest-energy (stable) solution, UHF#3, while each pair of degenerate eigenvalues leads to distinct stable solutions, UHF#1 and UHF#2 (see Table IV). The significant spin contamination of these UHF solutions, as indicated by the values of $\langle \hat{S}^2 \rangle$, reveals the spin frustration inherent in this system.

Figure 4 illustrates the Mulliken population analysis of the four stable HF solutions we have identified. The spin-σ electronic population on nucleus A is given by[212]

$$q_A^\sigma = -\sum_{\mu \in A} (\boldsymbol{P}^\sigma \cdot \boldsymbol{S})_{\mu\mu}, \tag{17}$$

where $\boldsymbol{P}^\sigma$ is the spin-σ density matrix and $\boldsymbol{S}$ is the overlap matrix, both expressed in the atomic orbital basis. A full half-circle represents an entire spin-up or spin-down electron located on this atom. In the RHF wave function, the spin-up and spin-down populations are identical, and the distribution of electrons on each site is nearly equal. However, in the UHF wave functions, electrons localize on specific centers, creating different patterns.

Transitioning from RHF to UHF results in a drastic improvement in the IP and EA estimates, highlighting the practical impact of breaking spatial and spin symmetries in the presence of spin frustration. However, determining which solution to favor in this case
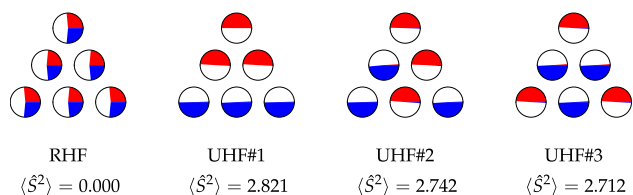
remains unclear: the lowest-energy solution with the largest spin contamination, UHF#3, is clearly inferior to the two others, while UHF#2 is slightly better for IPs but yields poor estimates of the EAs compared to UHF#1. These results highlight the practical challenges faced by GW calculations for molecules with severe multireference effects.

D. Dissociation of HF

Our final example deals with the dissociation of the HF molecule. Using Dunning's cc-pVDZ basis set, we compute the IP as a function of the internuclear distance R_{H-F} ranging from 0.5 to 3.5 Å at the FCI, HF, G_0W_0, and qsGW levels. Our results are reported in Fig. 5. Here, again, we employ both (stable) RHF and UHF starting points for the G_0W_0 and qsGW calculations. At equilibrium, the dominant closed-shell configuration is $|\cdots(3\sigma)^2(1\pi)^4\rangle$, while, at stretched geometries, two additional configurations, $|\cdots(1\pi^4)(4\sigma)^2\rangle$ and $|\cdots(1\pi^4)(3\sigma)(4\sigma)\rangle$, must be considered.

The FCI curve is rather simple: the IP decreases from a value of ~17 eV at $R_{H-F} = 0.5$ Å to reach a minimum of 13.3 eV around $R_{H-F} = 2$ Å before slightly increasing toward a limiting value of ~13.6 eV for large bond lengths. For small R_{H-F}, the RHF IP is a rather poor approximation of its FCI counterpart but follows the correct trend. In this regime, the G_0W_0 perturbative correction is

FIG. 4. Mulliken population analysis and the expectation values of $\hat{S}^2$ for the four HF solutions of the triangular-shaped H_6 cluster (see Table IV). A full half-circle corresponds to an entire spin-up or spin-down electron.
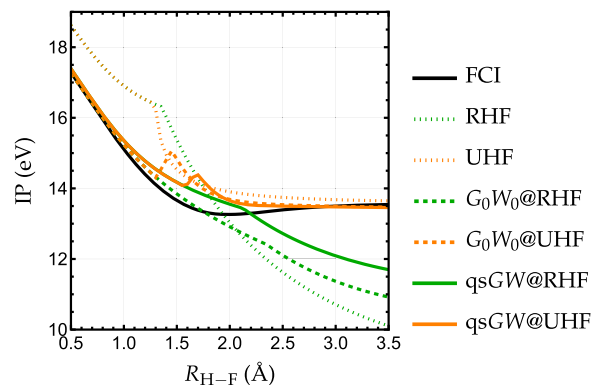

FIG. 5. Variation of the IP (in eV) of the HF molecule during its dissociation computed at various levels of theory. Restricted- and unrestricted-based calculations are represented in green and orange, respectively.

effective up to 1.5 Å. However, beyond this point, it deviates significantly. As observed previously, qsGW does not match the accuracy of G_0W_0 but follows a similar trend.

A UHF solution emerges around 1.4 Å, and the UHF IP provides an excellent estimate of the FCI value for large bond lengths, with a systematic improvement at both the G_0W_0 and qsGW levels. However, the transition between the RHF and UHF starting points results in non-smooth curves at the GW level, featuring bumps around the Coulson–Fischer point. Although this bump is mitigated at the qsGW level due to the self-consistency over the orbitals, it remains present. In this region, the self-consistent qsGW calculations are quite difficult to converge hinting at the presence of multiple solutions.[213–220] Apart from this, the qsGW@UHF curve accurately follows the FCI dissociation curve, providing a rather satisfactory description of this single-bond dissociation process.

V. CONCLUSION AND PERSPECTIVES

The present study highlights the diverse behavior of GW in the presence of strong correlation. For the Be + H_2 insertion reaction, the GW approximation provides a quantitative description, except in regions of strong multireference character, where the agreement is merely qualitative. For molecules with varying amounts of multireference character, the optimal compromise emerges with qsGW employing a symmetry-pure HF reference whenever available. This approach yields IP and EA estimates for both weakly and strongly correlated systems with notable accuracy. In contrast, the spin-frustrated H_6 cluster in a triangular arrangement and the dissociation of HF reveal that breaking spin symmetry is wise and useful in certain contexts. For the H_6 cluster, the RHF-based estimates exhibit significant deviations, whereas IPs and EAs obtained through qsGW with a UHF reference align much more closely with the FCI reference values. However, because various UHF solutions do exist, it is unclear which solution to favor in this case. Furthermore, the dissociation of the HF molecule demonstrates that self-consistency in addition to symmetry breaking can be useful for single-bond breaking processes, although the dissociation curve exhibits an unphysical "bump" near the Coulson–Fischer point. Scenarios involving multiple-bond breaking remain to be studied in this context.

Notably, the discrepancy in accuracy for different variants of GW and initial states is most pronounced for molecules that undergo spin-symmetry breaking at the Hartree–Fock level, including the spin-frustrated H_6 cluster and the dissociation of HF, and is relatively less severe in the two-configuration scenario of BeH_2. To overcome the challenges for spin-frustrated systems, we intend to explore the generalized version of GW, which allows the $\hat{S}_z$ symmetry to be broken, thus enabling the use of non-collinear reference wave functions for subsequent GW post-treatment. Strikingly, the accuracy remains acceptable in the case of B_2, despite its strong multireference character. This somewhat surprising result may be attributed to error compensation arising from the interplay between the level of self-consistency, the precise nature of the underlying mean-field solution, and the degree of multireference character.

We set out to investigate the accuracy of the GW approximation for multireference systems. Our findings indicate that, indeed, GW can describe such systems to a certain extent. However, it is clear that the errors are notably larger than those encountered in single-reference systems. While the precise relationship between the magnitude of this error and the number of dominant electronic configurations remains unexplored, this factor is an important avenue for future investigation. The absence of a universal estimator to quantify the degree of multireference character in a system makes it very difficult to determine the likelihood of GW failing. As a result, the nuanced performance of GW for multireference chemical systems emerges as the primary finding of our analysis. This conclusion resonates with findings in other fields, particularly within the context of solids.[221–225] Overall, GW has to be used with care and there is room to improve the accuracy of Green's function-based methods in systems with a strong multireference character. In this regard, the development of explicit multireference implementations,[226–230] although less black-box than the single-reference version, would be quite useful in certain chemical scenarios.

SUPPLEMENTARY MATERIAL

See the supplementary material for the specification of the basis set and the total energies for the Be + H_2 reaction, the total energies and additional G_0W_0 results of the set of multireference molecules, the geometry of the H_6 cluster, and the IP of the HF molecule as a function of the bond length.

AUTHOR DECLARATIONS

Conflict of Interest

The authors have no conflicts to disclose.

Author Contributions

Abdallah Ammar: Data curation (equal); Formal analysis (equal); Validation (equal); Writing – original draft (equal); Writing – review & editing (equal). **Antoine Marie**: Data curation (equal); Formal analysis (equal); Validation (equal); Writing – review & editing (equal). **Mauricio Rodríguez-Mayorga**: Data curation (equal); Formal analysis (equal); Software (equal); Validation (equal); Writing – review & editing (equal). **Hugh G. A. Burton**: Formal analysis (equal); Validation (equal); Writing – review & editing (equal). **Pierre-François Loos**: Conceptualization (equal); Data curation (equal); Formal analysis (equal); Funding acquisition (equal); Software (equal); Supervision (equal); Validation (equal); Writing – original draft (equal); Writing – review & editing (equal).

DATA AVAILABILITY

The data that support the findings of this study are available within the article and its supplementary material.

REFERENCES

[1]L. Hedin, Phys. Rev. 139, A796 (1965).

[2]R. M. Martin, L. Reining, and D. M. Ceperley, *Interacting Electrons: Theory and Computational Approaches* (Cambridge University Press, 2016).

[3]F. Aryasetiawan and O. Gunnarsson, Rep. Prog. Phys. 61, 237 (1998).

[4]G. Onida, L. Reining, and A. Rubio, Rev. Mod. Phys. 74, 601 (2002).

[5]L. Reining, Wiley Interdiscip. Rev.: Comput. Mol. Sci. 8, e1344 (2017).

[6]D. Golze, M. Dvorak, and P. Rinke, Front. Chem. 7, 377 (2019).

[7]A. Marie, A. Ammar, and P.-F. Loos, "The GW approximation: A quantum chemistry perspective," arXiv:2311.05351 [physics.chem-ph] (2023).

[8]X. Blase and C. Attaccalite, Appl. Phys. Lett. 99, 171909 (2011).

[9]J. Deslippe, G. Samsonidze, D. A. Strubbe, M. Jain, M. L. Cohen, and S. G. Louie, Comput. Phys. Commun. 183, 1269 (2012).

[10]X. Ren, P. Rinke, V. Blum, J. Wieferink, A. Tkatchenko, A. Sanfilippo, K. Reuter, and M. Scheffler, New J. Phys. 14, 053020 (2012).

[11]X. Blase, I. Duchemin, and D. Jacquemin, Chem. Soc. Rev. 47, 1022 (2018).

[12]I. Duchemin and X. Blase, J. Chem. Theory Comput. 16, 1742 (2020).

[13]I. Duchemin and X. Blase, J. Chem. Theory Comput. 17, 2383 (2021).

[14]F. Bruneval, T. Rangel, S. M. Hamed, M. Shao, C. Yang, and J. B. Neaton, Comput. Phys. Commun. 208, 149 (2016).

[15]M. J. van Setten, F. Weigend, and F. Evers, J. Chem. Theory Comput. 9, 232 (2013).

[16]F. Kaplan, F. Weigend, F. Evers, and M. J. van Setten, J. Chem. Theory Comput. 11, 5152 (2015).

[17]F. Kaplan, M. E. Harding, C. Seiler, F. Weigend, F. Evers, and M. J. van Setten, J. Chem. Theory Comput. 12, 2528 (2016).

[18]K. Krause and W. Klopper, J. Comput. Chem. 38, 383 (2017).

[19]A. Förster and L. Visscher, Phys. Rev. B 105, 125121 (2022).

[20]A. Förster and L. Visscher, J. Chem. Theory Comput. 18, 6779 (2022).

[21]A. Förster and L. Visscher, Front. Chem. 9, 736591 (2021).

[22]A. Förster and L. Visscher, J. Chem. Theory Comput. 16, 7381 (2020).

[23]F. Caruso, P. Rinke, X. Ren, M. Scheffler, and A. Rubio, Phys. Rev. B 86, 081102(R) (2012).

[24]F. Caruso, D. R. Rohr, M. Hellgren, X. Ren, P. Rinke, A. Rubio, and M. Scheffler, Phys. Rev. Lett. 110, 146403 (2013).

[25]F. Caruso, P. Rinke, X. Ren, A. Rubio, and M. Scheffler, Phys. Rev. B 88, 075105 (2013).

[26]F. Caruso, "Self-consistent GW approach for the unified description of ground and excited states of finite systems," PhD Thesis, Freie Universität Berlin, 2013.

[27]S. Iskakov, A. A. Rusakov, D. Zgid, and E. Gull, Phys. Rev. B 100, 085112 (2019).

[28]Q. Sun, X. Zhang, S. Banerjee, P. Bao, M. Barbry, N. S. Blunt, N. A. Bogdanov, G. H. Booth, J. Chen, Z.-H. Cui, J. J. Eriksen, Y. Gao, S. Guo, J. Hermann, M. R. Hermes, K. Koh, P. Koval, S. Lehtola, Z. Li, J. Liu, N. Mardirossian, J. D. McClain, M. Motta, B. Mussard, H. Q. Pham, A. Pulkin, W. Purwanto, P. J. Robinson, E. Ronca, E. R. Sayfutyarova, M. Scheurer, H. F. Schurkus, J. E. T. Smith, C. Sun, S.-N. Sun, S. Upadhyay, L. K. Wagner, X. Wang, A. White, J. D. Whitfield, M. J. Williamson, S. Wouters, J. Yang, J. M. Yu, T. Zhu, T. C. Berkelbach, S. Sharma, A. Y. Sokolov, and G. K.-L. Chan, J. Chem. Phys. 153, 024109 (2020).

[29]C. J. C. Scott, O. J. Backhouse, and G. H. Booth, J. Chem. Phys. 158, 124102 (2023).

[30]D. Neuhauser, E. Rabani, and R. Baer, J. Phys. Chem. Lett. 4, 1172 (2013).

[31]M. Govoni and G. Galli, J. Chem. Theory Comput. 11, 2680 (2015).

[32]P. Liu, M. Kaltak, J. c. v. Klimeš, and G. Kresse, Phys. Rev. B 94, 165109 (2016).

[33]V. Vlček, E. Rabani, D. Neuhauser, and R. Baer, J. Chem. Theory Comput. 13, 4997 (2017).

[34]J. Wilhelm, D. Golze, L. Talirz, J. Hutter, and C. A. Pignedoli, J. Phys. Chem. Lett. 9, 306 (2018).

[35]I. Duchemin and X. Blase, J. Chem. Phys. 150, 174120 (2019).

[36]M. D. Ben, F. H. da Jornada, A. Canning, N. Wichmann, K. Raman, R. Sasanka, C. Yang, S. G. Louie, and J. Deslippe, Comput. Phys. Commun. 235, 187 (2019).

[37]R. L. Panadés-Barrueta and D. Golze, J. Chem. Theory Comput. 19, 5450 (2023).

[38]M. J. van Setten, F. Caruso, S. Sharifzadeh, X. Ren, M. Scheffler, F. Liu, J. Lischner, L. Lin, J. R. Deslippe, S. G. Louie, C. Yang, F. Weigend, J. B. Neaton, F. Evers, and P. Rinke, J. Chem. Theory Comput. 11, 5665 (2015).

[39]N. Marom, F. Caruso, X. Ren, O. T. Hofmann, T. Körzdörfer, J. R. Chelikowsky, A. Rubio, M. Scheffler, and P. Rinke, Phys. Rev. B 86, 245127 (2012).

[40]J. W. Knight, X. Wang, L. Gallandi, O. Dolgounitcheva, X. Ren, J. V. Ortiz, P. Rinke, T. Körzdörfer, and N. Marom, J. Chem. Theory Comput. 12, 615 (2016).

[41]F. Caruso, M. Dauth, M. J. van Setten, and P. Rinke, J. Chem. Theory Comput. 12, 5076 (2016).

[42]E. Maggio, P. Liu, M. J. van Setten, and G. Kresse, J. Chem. Theory Comput. 13, 635 (2017).

[43]M. Govoni and G. Galli, J. Chem. Theory Comput. 14, 1895 (2018).

[44]N. Colonna, N. L. Nguyen, A. Ferretti, and N. Marzari, J. Chem. Theory Comput. 15, 1905 (2019).

[45]D. Golze, L. Keller, and P. Rinke, J. Phys. Chem. Lett. 11, 1840 (2020).

[46]A. Stuke, C. Kunkel, D. Golze, M. Todorović, J. T. Margraf, K. Reuter, P. Rinke, and H. Oberhofer, Sci. Data 7, 58 (2020).

[47]M. Rohlfing and S. G. Louie, Phys. Rev. Lett. 82, 1959 (1999).

[48]J.-W. van der Horst, P. A. Bobbert, M. A. J. Michels, G. Brocks, and P. J. Kelly, Phys. Rev. Lett. 83, 4413 (1999).

[49]P. Puschnig and C. Ambrosch-Draxl, Phys. Rev. Lett. 89, 056405 (2002).

[50]M. L. Tiago, J. E. Northrup, and S. G. Louie, Phys. Rev. B 67, 115212 (2003).

[51]D. Rocca, D. Lu, and G. Galli, J. Chem. Phys. 133, 164109 (2010).

[52]P. Boulanger, D. Jacquemin, I. Duchemin, and X. Blase, J. Chem. Theory Comput. 10, 1212 (2014).

[53]D. Jacquemin, I. Duchemin, and X. Blase, J. Chem. Theory Comput. 11, 3290 (2015).

[54]F. Bruneval, S. M. Hamed, and J. B. Neaton, J. Chem. Phys. 142, 244101 (2015).

[55]D. Jacquemin, I. Duchemin, and X. Blase, J. Chem. Theory Comput. 11, 5340 (2015).

[56]D. Hirose, Y. Noguchi, and O. Sugino, Phys. Rev. B 91, 205111 (2015).

[57]D. Jacquemin, I. Duchemin, and X. Blase, J. Phys. Chem. Lett. 8, 1524 (2017).

[58]D. Jacquemin, I. Duchemin, A. Blondel, and X. Blase, J. Chem. Theory Comput. 13, 767 (2017).

[59]T. Rangel, S. M. Hamed, F. Bruneval, and J. B. Neaton, J. Chem. Phys. 146, 194108 (2017).

[60]X. Gui, C. Holzer, and W. Klopper, J. Chem. Theory Comput. 14, 2127 (2018).

[61]C. Liu, J. Kloppenburg, Y. Yao, X. Ren, H. Appel, Y. Kanai, and V. Blum, J. Chem. Phys. 152, 044105 (2020).

[62]X. Blase, I. Duchemin, D. Jacquemin, and P.-F. Loos, J. Phys. Chem. Lett. 11, 7371 (2020).

[63]C. Holzer and W. Klopper, J. Chem. Phys. 149, 101101 (2018).

[64]C. Holzer, X. Gui, M. E. Harding, G. Kresse, T. Helgaker, and W. Klopper, J. Chem. Phys. 149, 144106 (2018).

[65]P.-F. Loos, A. Scemama, I. Duchemin, D. Jacquemin, and X. Blase, J. Phys. Chem. Lett. 11, 3536 (2020).

[66]P.-F. Loos, M. Comin, X. Blase, and D. Jacquemin, J. Chem. Theory Comput. 17, 3666 (2021).

[67]E. Monino and P.-F. Loos, J. Chem. Theory Comput. 17, 2852 (2021).

[68]C. A. McKeon, S. M. Hamed, F. Bruneval, and J. B. Neaton, J. Chem. Phys. 157, 074103 (2022).

[69]E. Monino and P.-F. Loos, J. Chem. Phys. 159, 034105 (2023).

[70]E. E. Salpeter and H. A. Bethe, Phys. Rev. 84, 1232 (1951).

[71]G. Strinati, Riv. Nuovo Cim. 11, 1 (1988).

[72]F. Bruneval, N. Dattani, and M. J. van Setten, Front. Chem. 9, 749779 (2021).

[73]C. Verdozzi, R. W. Godby, and S. Holloway, Phys. Rev. Lett. 74, 2327 (1995).

[74]S. Di Sabatino, J. A. Berger, L. Reining, and P. Romaniello, Phys. Rev. B 94, 155141 (2016).

[75]J. M. Tomczak, P. Liu, A. Toschi, G. Kresse, and K. Held, Eur. Phys. J.: Spec. Top. 226, 2565 (2017).

[76] M. Dvorak and P. Rinke, Phys. Rev. B **99**, 115134 (2019).

[77] M. Dvorak, D. Golze, and P. Rinke, Phys. Rev. Mater. **3**(7), 070801 (2019).

[78] S. Di Sabatino, J. Koskelo, J. A. Berger, and P. Romaniello, Phys. Rev. B **105**, 235123 (2022).

[79] S. Di Sabatino, J. Koskelo, J. A. Berger, and P. Romaniello, Phys. Rev. B **107**, 035111 (2023).

[80] R. Orlando, P. Romaniello, and P.-F. Loos, J. Chem. Phys. **159**, 184113 (2023).

[81] M. Gell-Mann and K. A. Brueckner, Phys. Rev. **106**, 364 (1957).

[82] R. D. Mattuck, *A Guide to Feynman Diagrams in the Many-Body Problem*, 2nd ed., Dover Books on Physics and Chemistry (Dover Publications, New York, 1992).

[83] D. Bohm and D. Pines, Phys. Rev. **82**, 625 (1951).

[84] D. Pines and D. Bohm, Phys. Rev. **85**, 338 (1952).

[85] D. Bohm and D. Pines, Phys. Rev. **92**, 609 (1953).

[86] P. Nozières and D. Pines, Phys. Rev. **111**, 442 (1958).

[87] G. E. Scuseria, T. M. Henderson, and D. C. Sorensen, J. Chem. Phys. **129**, 231101 (2008).

[88] M. F. Lange and T. C. Berkelbach, J. Chem. Theory Comput. **14**, 4224 (2018).

[89] J. Tölle and G. Kin-Lic Chan, J. Chem. Phys. **158**, 124123 (2023).

[90] N. F. Mott, Proc. Phys. Soc. A **62**, 416 (1949).

[91] M. Imada, A. Fujimori, and Y. Tokura, Rev. Mod. Phys. **70**, 1039 (1998).

[92] J. Hubbard, Proc. Math. Phys. Eng. **276**, 238 (1963).

[93] E. H. Lieb and F. Wu, Phys. Rev. Lett. **20**, 1445 (1968).

[94] A. Montorsi, *The Hubbard Model: A Reprint Volume* (World Scientific, 1992).

[95] G. F. Giuliani and G. Vignale, *Quantum Theory of Electron Liquid* (Cambridge University Press, Cambridge, England, 2005).

[96] P.-F. Loos and P. M. W. Gill, WIREs Comput. Mol. Sci. **6**, 410 (2016).

[97] E. Wigner, Phys. Rev. **46**, 1002 (1934).

[98] G. Baym and L. P. Kadanoff, Phys. Rev. **124**, 287 (1961).

[99] G. Baym, Phys. Rev. **127**, 1391 (1962).

[100] P. Danielewicz, Ann. Phys. **152**, 239 (1984).

[101] P. Danielewicz, Ann. Phys. **152**, 305 (1984).

[102] C. Barbieri, D. Van Neck, and W. H. Dickhoff, Phys. Rev. A **76**, 052503 (2007).

[103] W. H. DickHoff and D. V. Neck, *Many-body Theory Exposed!* (World Sientific, 2008).

[104] P. Romaniello, F. Bechstedt, and L. Reining, Phys. Rev. B **85**, 155131 (2012).

[105] D. Zhang, N. Q. Su, and W. Yang, J. Phys. Chem. Lett. **8**, 3223 (2017).

[106] J. Li, Z. Chen, and W. Yang, J. Phys. Chem. Lett. **12**, 6203 (2021).

[107] P.-F. Loos and P. Romaniello, J. Chem. Phys. **156**, 164101 (2022).

[108] J. Li, J. Yu, Z. Chen, and W. Yang, J. Phys. Chem. A **127**, 7811 (2023).

[109] R. Orlando, P. Romaniello, and P.-F. Loos, "Exploring new exchange-correlation kernels in the Bethe–Salpeter equation: A study of the asymmetric Hubbard dimer," *Advances in Quantum Chemistry* (Elsevier, 2023), pp. 183–211.

[110] Y. Yang, H. van Aggelen, S. N. Steinmann, D. Peng, and W. Yang, J. Chem. Phys. **139**, 104112 (2013).

[111] G. E. Scuseria, T. M. Henderson, and I. W. Bulik, J. Chem. Phys. **139**, 104113 (2013).

[112] T. C. Berkelbach, J. Chem. Phys. **149**, 041103 (2018).

[113] R. Del Sole, L. Reining, and R. W. Godby, Phys. Rev. B **49**, 8024 (1994).

[114] E. L. Shirley, Phys. Rev. B **54**, 7758 (1996).

[115] A. Schindlmayr and R. W. Godby, Phys. Rev. Lett. **80**, 1702 (1998).

[116] A. J. Morris, M. Stankovski, K. T. Delaney, P. Rinke, P. García-González, and R. W. Godby, Phys. Rev. B **76**, 155106 (2007).

[117] M. Shishkin, M. Marsman, and G. Kresse, Phys. Rev. Lett. **99**, 246403 (2007).

[118] P. Romaniello, S. Guyot, and L. Reining, J. Chem. Phys. **131**, 154111 (2009).

[119] A. Grüneis, G. Kresse, Y. Hinuma, and F. Oba, Phys. Rev. Lett. **112**, 096401 (2014).

[120] L. Hung, F. Bruneval, K. Baishya, and S. Öğüt, J. Chem. Theory Comput. **13**, 2135 (2017).

[121] E. Maggio and G. Kresse, J. Chem. Theory Comput. **13**, 4765 (2017).

[122] B. Cunningham, M. Grüning, P. Azarhoosh, D. Pashov, and M. van Schilfgaarde, Phys. Rev. Mater. **2**, 034603 (2018).

[123] V. Vlček, J. Chem. Theory Comput. **15**, 6254 (2019).

[124] A. M. Lewis and T. C. Berkelbach, J. Chem. Theory Comput. **15**, 2925 (2019).

[125] Y. Pavlyukh, G. Stefanucci, and R. van Leeuwen, Phys. Rev. B **102**, 045121 (2020).

[126] Y. Wang, P. Rinke, and X. Ren, J. Chem. Theory Comput. **17**, 5140 (2021).

[127] C. Mejuto-Zaera, G. Weng, M. Romanova, S. J. Cotton, K. B. Whaley, N. M. Tubman, and V. Vlček, J. Chem. Phys. **154**, 121101 (2021).

[128] C. Mejuto-Zaera and V. c. v. Vlček, Phys. Rev. B **106**, 165129 (2022).

[129] Y. Wang and X. Ren, J. Chem. Theory Comput. **157**, 214115 (2022).

[130] G. Weng, R. Mallarapu, and V. Vlček, J. Chem. Phys. **158**, 144105 (2023).

[131] C. E. Shannon, Bell Syst. Tech. J. **27**, 379 (1948).

[132] I. M. Nielsen and C. L. Janssen, Chem. Phys. Lett. **310**, 568 (1999).

[133] V. V. Ivanov, D. I. Lyakh, and L. Adamowicz, Mol. Phys. **103**, 2131 (2005).

[134] U. R. Fogueri, S. Kozuch, A. Karton, and J. M. L. Martin, Theor. Chem. Acc. **132**, 1291 (2012).

[135] E. Ramos-Cordoba, P. Salvador, and E. Matito, Phys. Chem. Chem. Phys. **18**, 24015 (2016).

[136] R. J. Bartlett, Y. C. Park, N. P. Bauman, A. Melnichuk, D. Ranasinghe, M. Ravi, and A. Perera, J. Chem. Phys. **153**, 234103 (2020).

[137] X. Xu, L. Soriano-Agueda, X. López, E. Ramos-Cordoba, and E. Matito, J. Chem. Theory Comput. **20**(2), 721 (2024).

[138] G. D. Purvis III, R. Shepard, F. B. Brown, and R. J. Bartlett, Int. J. Quantum Chem. **23**, 835 (1983).

[139] R. J. Gdanitz and R. Ahlrichs, Chem. Phys. Lett. **143**, 413 (1988).

[140] U. S. Mahapatra, B. Datta, B. Bandyopadhyay, and D. Mukherjee, *Advances in Quantum Chemistry* (Academic Press, 1998), Vol. 130.

[141] U. S. Mahapatra, B. Datta, and D. Mukherjee, J. Chem. Phys. **110**, 6171 (1999).

[142] S. B. Sharp and G. I. Gellene, J. Phys. Chem. A **104**, 10951 (2000).

[143] M. Kállay, P. G. Szalay, and P. R. Surján, J. Chem. Phys. **117**, 980 (2002).

[144] J. Pittner, H. V. Gonzalez, R. J. Gdanitz, and P. Čársky, Chem. Phys. Lett. **386**, 211 (2004).

[145] P. J. A. Ruttink, J. H. V. Lenthe, and P. Todorov, Mol. Phys. **103**, 2497 (2005).

[146] D. I. Lyakh, V. V. Ivanov, and L. Adamowicz, Theor. Chem. Acc. **116**, 427 (2006).

[147] T. Yanai and G. K.-L. Chan, J. Chem. Phys. **124**, 194106 (2006).

[148] F. A. Evangelista and J. Gauss, J. Chem. Phys. **134**, 114102 (2011).

[149] F. A. Evangelista and J. Gauss, J. Chem. Phys. **134**, 224102 (2011).

[150] F. A. Evangelista, M. Hanauer, A. Köhn, and J. Gauss, J. Chem. Phys. **136**, 204108 (2012).

[151] C. W. Bauschlicher, S. R. Langhoff, P. R. Taylor, N. C. Handy, and P. J. Knowles, J. Chem. Phys. **85**, 1469 (1986).

[152] K. A. Peterson and T. H. Dunning, J. Chem. Phys. **102**, 2032 (1995).

[153] K. B. Ghose, P. Piecuch, and L. Adamowicz, J. Chem. Phys. **103**, 9331 (1995).

[154] X. Li and J. Paldus, J. Chem. Phys. **108**, 637 (1998).

[155] A. I. Krylov, C. D. Sherrill, E. F. C. Byrd, and M. Head-Gordon, J. Chem. Phys. **109**, 10669 (1998).

[156] V. V. Ivanov, L. Adamowicz, and D. I. Lyakh, J. Mol. Struc.: THEOCHEM **768**, 97 (2006).

[157] A. Engels-Putzka and M. Hanrath, J. Mol. Struc.: THEOCHEM **902**, 59 (2009).

[158] S. Das, D. Mukherjee, and M. Kállay, J. Chem. Phys. **132**, 074103 (2010).

[159] G. Csanak, H. Taylor, and R. Yaris, *Advances in Atomic and Molecular Physics* (Elsevier, 1971), Vol. 7, pp. 287–361.

[160] A. L. Fetter and J. D. Walecka, *Quantum Theory of Many Particle Systems* (McGraw Hill, San Francisco, 1971).

[161] R. Starke and G. Kresse, Phys. Rev. B **85**, 075119 (2012).

[162] G. Strinati, H. J. Mattausch, and W. Hanke, Phys. Rev. Lett. **45**, 290 (1980).

[163] M. S. Hybertsen and S. G. Louie, Phys. Rev. Lett. **55**, 1418 (1985).

[164] R. W. Godby, M. Schlüter, and L. J. Sham, Phys. Rev. B **37**, 10159 (1988).

[165] W. von der Linden and P. Horsch, Phys. Rev. B **37**, 8351 (1988).

[166] J. E. Northrup, M. S. Hybertsen, and S. G. Louie, Phys. Rev. Lett. **66**, 500 (1991).

[167] X. Blase, X. Zhu, and S. G. Louie, Phys. Rev. B **49**, 4973 (1994).

[168] M. Rohlfing, P. Krüger, and J. Pollmann, Phys. Rev. B **52**, 1905 (1995).

[169] M. S. Hybertsen and S. G. Louie, Phys. Rev. B **34**, 5390 (1986).

[170] M. Shishkin and G. Kresse, Phys. Rev. B **75**, 235102 (2007).

[171] C. Faber, C. Attaccalite, V. Olevano, E. Runge, and X. Blase, Phys. Rev. B **83**, 115123 (2011).

[172] T. Rangel, S. M. Hamed, F. Bruneval, and J. B. Neaton, J. Chem. Theory Comput. **12**, 2834 (2016).

[173] S. V. Faleev, M. van Schilfgaarde, and T. Kotani, Phys. Rev. Lett. **93**, 126406 (2004).

[174] M. van Schilfgaarde, T. Kotani, and S. Faleev, Phys. Rev. Lett. **96**, 226402 (2006).

[175] T. Kotani, M. van Schilfgaarde, and S. V. Faleev, Phys. Rev. B **76**, 165106 (2007).

[176] S.-H. Ke, Phys. Rev. B **84**, 205415 (2011).

[177] A. Marie and P.-F. Loos, J. Chem. Theory Comput. **19**, 3943 (2023).

[178] Y. Garniron, T. Applencourt, K. Gasperich, A. Benali, A. Ferté, J. Paquier, B. Pradines, R. Assaraf, P. Reinhardt, J. Toulouse, P. Barbaresco, N. Renon, G. David, J. P. Malrieu, M. Véril, M. Caffarel, P. F. Loos, E. Giner, and A. Scemama, J. Chem. Theory Comput. **15**, 3591 (2019).

[179] B. Huron, J. P. Malrieu, and P. Rancurel, J. Chem. Phys. **58**, 5745 (1973).

[180] E. Giner, A. Scemama, and M. Caffarel, Can. J. Chem. **91**, 879 (2013).

[181] E. Giner, A. Scemama, and M. Caffarel, J. Chem. Phys. **142**, 044115 (2015).

[182] Y. Garniron, A. Scemama, P.-F. Loos, and M. Caffarel, J. Chem. Phys. **147**, 034101 (2017).

[183] Y. Garniron, A. Scemama, E. Giner, M. Caffarel, and P. F. Loos, J. Chem. Phys. **149**, 064103 (2018).

[184] R. Seeger and J. A. Pople, J. Chem. Phys. **66**, 3045 (1977).

[185] H. Fukutome, Int. J. Quantum Chem. **20**, 955 (1981).

[186] J. Stuber and J. Paldus, "Symmetry breaking in the independent particle model," in *Fundamental World of Quantum Chemistry: A Tribute to the Memory of Per-Olov Löwdin*, edited by E. J. Brändas and E. S. Kryachko (Kluwer Academic, Dordrecht, 2003), Vol. 1, p. 67.

[187] E. L. Shirley and R. M. Martin, Phys. Rev. B **47**, 15404 (1993).

[188] S. Yamanaka, Y. Shigeta, Y. Ohta, D. Yamaki, H. Nagao, and K. Yamaguchi, Int. J. Quantum Chem. **84**, 369 (2001).

[189] M. Mansouri, D. Casanova, P. Koval, and D. Sánchez-Portal, New J. Phys. **23**, 093027 (2021).

[190] P. Pokhilko and D. Zgid, J. Chem. Phys. **157**, 144101 (2022).

[191] P. Pokhilko and D. Zgid, J. Phys. Chem. Lett. **14**, 5777 (2023).

[192] H. G. A. Burton and A. J. W. Thom, J. Chem. Theory Comput. **12**, 167 (2016).

[193] H. G. A. Burton, M. Gross, and A. J. W. Thom, J. Chem. Theory Comput. **14**, 607 (2018).

[194] A. Marie, H. G. A. Burton, and P.-F. Loos, J. Phys.: Condens.Matter **33**, 283001 (2021).

[195] D. K. W. Mok, R. Neumann, and N. C. Handy, J. Phys. Chem. **100**, 6225 (1996).

[196] K. P. Huber and G. Herzberg, *Molecular Spectra and Molecular Structure: IV. Constants of Diatomic Molecules* (van Nostrand Reinhold Company, 1979).

[197] F. Weigend and R. Ahlrichs, Phys. Chem. Chem. Phys. **7**, 3297 (2005).

[198] W. R. M. Graham and W. Weltner, J. Chem. Phys. **65**, 1516 (1976).

[199] M. Dupuis and B. Liu, J. Chem. Phys. **68**, 2902 (1978).

[200] P. Deutsch, L. Curtiss, and J. Pople, Chem. Phys. Lett. **174**, 33 (1990).

[201] P. J. Bruna and J. S. Wright, J. Phys. Chem. **94**, 1774 (1990).

[202] C. W. Bauschlicher, S. R. Langhoff, and S. R. Langhoff, J. Chem. Phys. **87**, 2919 (1987).

[203] M. L. Abrams and C. D. Sherrill, J. Chem. Phys. **121**, 9211 (2004).

[204] C. D. Sherrill and P. Piecuch, J. Chem. Phys. **122**, 124104 (2005).

[205] X. Li and J. Paldus, Chem. Phys. Lett. **431**, 179 (2006).

[206] G. H. Booth, D. Cleland, A. J. W. Thom, and A. Alavi, J. Chem. Phys. **135**, 084104 (2011).

[207] M. Lorenz, J. Agreiter, A. M. Smith, and V. E. Bondybey, J. Chem. Phys. **104**, 3143 (1996).

[208] A. D. Becke, Phys. Rev. A **38**, 3098 (1988).

[209] C. Lee, W. Yang, and R. G. Parr, Phys. Rev. B **37**, 785 (1988).

[210] A. D. Becke, J. Chem. Phys. **98**, 5648 (1993).

[211] T. Yanai, D. P. Tew, and N. C. Handy, Chem. Phys. Lett. **393**, 51 (2004).

[212] A. Szabo and N. S. Ostlund, *Modern Quantum Chemistry* (McGraw-Hill, New York, 1989).

[213] P. F. Loos, P. Romaniello, and J. A. Berger, J. Chem. Theory Comput. **14**, 3071 (2018).

[214] M. Véril, P. Romaniello, J. A. Berger, and P. F. Loos, J. Chem. Theory Comput. **14**, 5220 (2018).

[215] P. Pokhilko and D. Zgid, J. Chem. Phys. **155**, 024101 (2021).

[216] P. Pokhilko, S. Iskakov, C.-N. Yeh, and D. Zgid, J. Chem. Phys. **155**, 024119 (2021).

[217] J. A. Berger, P.-F. Loos, and P. Romaniello, J. Chem. Theory Comput. **17**, 191 (2020).

[218] S. Di Sabatino, P.-F. Loos, and P. Romaniello, Front. Chem. **9**, 751054 (2021).

[219] P. Pokhilko, C.-N. Yeh, and D. Zgid, J. Chem. Phys. **156**, 094101 (2022).

[220] E. Monino and P.-F. Loos, J. Chem. Phys. **156**, 231101 (2022).

[221] S. Kobayashi, Y. Nohara, S. Yamamoto, and T. Fujiwara, Phys. Rev. B **78**, 155112 (2008).

[222] H. Jiang, R. I. Gomez-Abal, P. Rinke, and M. Scheffler, Phys. Rev. Lett. **102**, 126403 (2009).

[223] H. Jiang, R. I. Gomez-Abal, P. Rinke, and M. Scheffler, Phys. Rev. B **82**, 045108 (2010).

[224] J. M. Tomczak, M. van Schilfgaarde, and G. Kotliar, Phys. Rev. Lett. **109**, 237010 (2012).

[225] M. Gatti and M. Guzzo, Phys. Rev. B **87**, 155147 (2013).

[226] C. Brouder, G. Panati, and G. Stoltz, Phys. Rev. Lett. **103**, 230401 (2009).

[227] E. Linnér and F. Aryasetiawan, Phys. Rev. B **100**, 235106 (2019).

[228] A. Y. Sokolov, J. Chem. Phys. **149**, 204113 (2018).

[229] K. Chatterjee and A. Y. Sokolov, J. Chem. Theory Comput. **15**, 5908 (2019).

[230] K. Chatterjee and A. Y. Sokolov, J. Chem. Theory Comput. **16**, 6343 (2020).